

Proceeding to the LHC seminar talk *Update of the $B^0 \rightarrow K^{*0} \mu^+ \mu^-$ angular analysis at LHCb* held by Eluned Smith on behalf of the LHC collaboration on 13th of March 2020.

Nils Breer

Technische Universität Dortmund

The stated Process is of such importance because the $b \rightarrow s\mu\mu$ transition is forbidden at tree level due to FCNC and can only occur at loop order. Because of that, these processes are much more sensitive to new physics(NP).

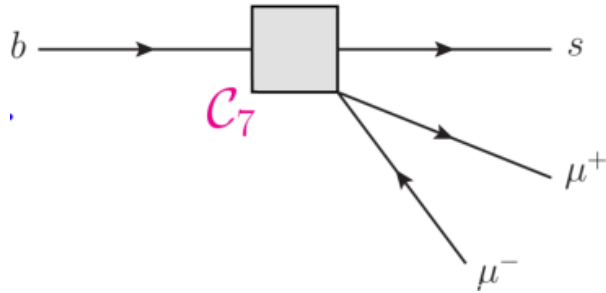


Figure 1: Wilson coefficient C_7 in .

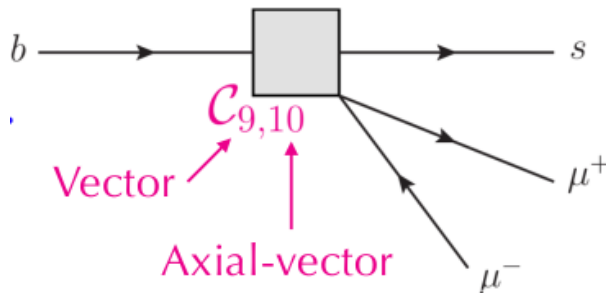


Figure 2: Process in new physics model.

To gather information about short distance NP above the SM energy scale μ , wilson coefficients $C_i(\mu)$ and low-energy QCD Operators O_i are used to describe that.

The wilson coefficients C_7 , C_9 and C_{10} are of great importance since observables like the forward-backward asymmetry and P_5' are sensitive for C_9 especially.

In an effective theory, C_9 and C_{10} are used to describe the contribution from loops, in which

electroweak gauge bosons are produced. wilson coefficient C_7 describes the contribution from loopdiagramms which produce photons from the loops.

This can be summarized by an effective hamiltonian

$$H_{eff} = -\frac{4G_f}{\sqrt{2}} V_{tb} V_{ts}^* \sum_i C_i \cdot O_i + \text{h.c.}$$

G_F is Fermi's constant, μ ist the renormalization scale, $V_{tb} V_{ts}^*$ is the contains leading flavor factors of the SM which lie in the CKM matrix elements V_{ij}

To measure the decay rate as a function of angles of the decay products, an angular analysis is performed. The definition of the angular observables θ_k , θ_l and ϕ is schematically shown in figure 3

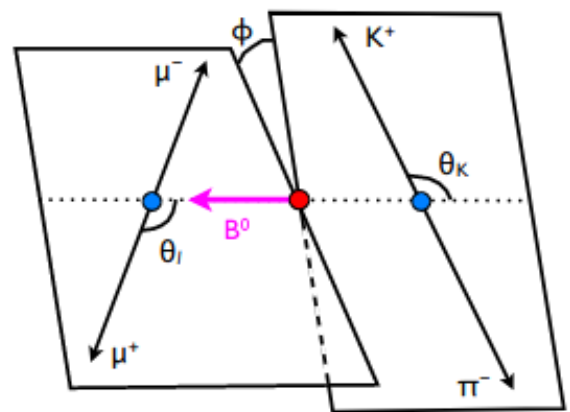


Figure 3: image of the angular observables.[3]

In this analysis, the forward-backard asymmetry A_{FB} , F_L the fraction of the longitudinal polarisation of the K^{*0} and the decay rate of the process $B^0 \rightarrow K^{*0} \mu\mu$ was measured. The

definition of the angular observables are the following. θ_l is the angle between the negatively charged lepton and \bar{B} in the dimuon center of mass system (c.m.s). θ_k is the angle between the Kaon and the \bar{B} in the K^{*0} c.m.s.. The angle between the K^{*0} -plane and the dimuon-plane is defined by the angle ϕ [2].

Considering that S-wave contribution, spinless $K^+\pi^-$ constellations, can pollute the measurement, therefore a parametrization such as $(1 - F_S)$ for this was taken into account where $(1 - F_S)$ is the S-wave fraction which describes the amount of S-wave contribution. The interference Amplitude between P-wave and S-wave decays are parametrized by A_S . The angular distribution[3] for the $B^0 \rightarrow K^{*0}\mu\mu$ decay reads

$$\frac{1}{\Gamma} \frac{d^3\Gamma}{d\theta_k d\theta_l dq^2} = f(F_S, A_S, \theta_k, \theta_l, A_{FB}, F_L)$$

Since A_{FB} , F_L and $\mathcal{A} \times E$ do not depend on the angle ϕ , it is already integrated out. The angular description for The B and \bar{B} are combined afterwards and expanded into a sum of the angular variables multiplied with a fitparameter, which are the A_{FB} , F_L and S_i , which are called CP-averaged observables because they contain CP violation.

$$\frac{1}{d(\Gamma + \bar{\Gamma})/dq^2 d\cos\theta_l d\cos\theta_K d\phi} \bigg|_P = \frac{9}{32\pi} \left[\frac{3}{4} (1 - F_L) \sin^2 \theta_K + F_L \cos^2 \theta_K + \frac{1}{4} (1 - F_L) \sin^2 \theta_K \cos 2\theta_l - F_L \cos^2 \theta_K \cos 2\theta_l + S_3 \sin^2 \theta_K \sin^2 \theta_l \cos 2\phi + S_4 \sin 2\theta_K \sin 2\theta_l \cos \phi + S_5 \sin 2\theta_K \sin \theta_l \cos \phi + \frac{3}{4} A_{FB} \sin^2 \theta_K \cos \theta_l + S_7 \sin 2\theta_K \sin \theta_l \sin \phi + S_8 \sin 2\theta_K \sin 2\theta_l \sin \phi + S_9 \sin^2 \theta_K \sin^2 \theta_l \sin 2\phi \right]$$

F_L : fraction of longitudinal polarisation of the K^{*0}
 A_{FB} : forward-backward asymmetry of dimuon system

Figure 4: Angular description for B and \bar{B} combined.

Then the fit in the S_i basis was reparametrised to the P_i basis. This was done to eliminate first order uncertainties in the form factors primarily. The fit yields seven CP violating observables including F_L .

$$P_1 = \frac{2S_3}{1 - F_L} \quad P_{4,5,8}' = \frac{S_{4,5,8}}{\sqrt{F_L(1 - F_L)}} \\ P_2 = \frac{2}{3} \frac{A_{FB}}{1 - F_L} \quad P_6' = \frac{S_7}{\sqrt{F_L(1 - F_L)}} \\ P_3 = \frac{-S_9}{1 - F_L}$$

This analysis especially focuses heavily on the tension induced by P_5' , since it is a very sensitive variable for C_9 . This can be seen in the range of $4 - 8 \frac{\text{GeV}}{c^4}$. For every collaboration a discrepancy of between the SM and the measurement displayed in figure 5

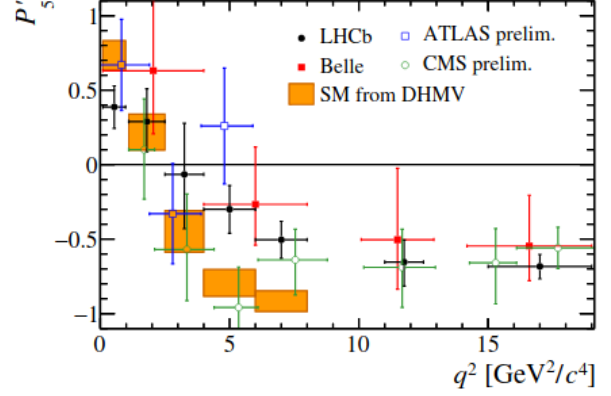


Figure 5: tension in P_5' . [1]

Angular analysis for local tension in P_5' performed by other collaborations such as ATLAS and CMS show similar results but Data taken stops at roughly the $J\psi$ Mass due to the resonant background. Therefore the ATLAS measurement is not so good. As seen in some global fits, the shift in the wilson coefficient $\text{Re}(C_9)$, the deviations in these wilson coefficients or up to $3 - 5 \sigma$. In general, these fits are a good tool to learn from the fits.

The data used comes from the years 2011, 2012, which was Run 1, and 2016. The center of mass energies were 7, 8 and 13 TeV respectively. The data taken in the later years is nearly double from what the have taken in 2011.

For the stated process, it is required that the impact parameter for the daughters are quite large because they don't come from the primary vertex. Also the PID¹ is used to suppress the peaks in the background. Machine learning algorithms are used to reduce combinatorial background. For the probe regions in the q^2 plot, the signal regions must be separated from the background regions. Since there are decay modes which have the same final state as our wanted process, there are several peak regions which must be cut out. This is for example the charmonium background of the $J\psi$ and the ψ

¹particle identification

meson. The signal regions for the decay mode $b \rightarrow s\mu\mu$ can be interpreted separately. Also the photon pole at $q^2 = 0$ can be examined. The binning used is historically conditioned. The only cause for that is to compact the data. One boundary at 1.1 GeV is set to delete the $\phi(1020)$ resonance from the data.

To describe now the physics behind the angular analysis, instead of using the non-perturbative QCD form factors and the wilson coefficients, angular amplitudes A^{LR} are defined. Then we measure in the bins of $q^2 = m^2(\mu\mu)$ by firstly integrating over q^2 and secondly combining this with the B^0 and \bar{B}^0 decays. This results in a so called CP-averaged basis S_i . The resulting $\frac{d\Gamma}{dq^2}$ spectrum is then

$$\frac{1}{\frac{d(\Gamma+\bar{\Gamma})}{dq^2}} \cdot \frac{d(\Gamma+\bar{\Gamma})}{d\cos\theta_l d\cos\theta_k d\phi} \Big|_P = \frac{9}{32\pi} \cdot f(F_L, \theta_k, \theta_l, A_{FB}, S_i)$$

Here, the F_L describes the fraction of longitudinal polarisation of the K^{0*} . A_{FB} is the forward/backward asymmetry of the dimuon system. In order to reduce uncertainties, the first basis of the S_i is transformed into a basis P_i which takes ratios of observables[4]. In the full fit model the shape of the invariant mass plots are used to determine the amount of signal and background in the data.

$$\text{PDF}_{total} = f_{sig} \text{PDF}_{sig}(\vec{\Omega}, m) + (1 - f_{sig}) \text{PDF}_{bkg}$$

The PDF function can be separated into an angular part and a massive part. After that a maximum likelihood fit is performed. As seen in figure 6 the massive part of the signal PDF is a gaussian function with a radiative tail and the background PDF results in a exponential function.

Because of the factorization of the signal and background PDF

$$\text{PDF}_{sig}(\vec{\Omega}, m) = \text{PDF}_{sig}(\vec{\Omega}) \times \text{PDF}_{sig}(m)$$

the angular part of the signal PDF of the Run 1 data and the data from 2016 can be shared in the analysis to perform a simultaneous fit $\sum_I S_{i,q_{bin}^2} f_i(\Omega)$.

Because the angular distribution and the q^2 distribution are influenced by the efficiencies, the parametrisation must be well known. This is

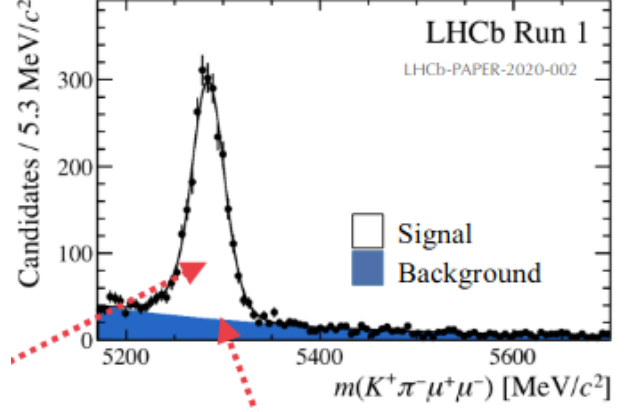


Figure 6: invariant B mass of Run 1 LHCb data.

done via an acceptance function, here the Legendre polynomials. With 3 angles and q^2 a 4D parametrisation results in 4 coefficients

The $K\pi$ final state has more than one spin eigenstate. Therefore, additional terms are needed to differentiate between these states. Because $K\pi\mu\mu$ can be produced in a vector state which disturbs the angular distribution, the different structures of the spin 1 K^{0*} and the flat structure of the $K\pi$ state need to be analyzed.

The dominant systematic uncertainties across the q^2 bins are acceptance variation with q^2 , peaking backgrounds and the bias correction. The whole table of uncertainties is shown in figure 7[4].

Source	F_L	S_3-S_9	$P_1-P'_8$
Acceptance stat. uncertainty	< 0.01	< 0.01	< 0.01
Acceptance polynomial order	< 0.01	< 0.01	< 0.02
Data-simulation differences	< 0.01	< 0.01	< 0.01
Acceptance variation with q^2	< 0.03	< 0.01	< 0.09
$m(K^+\pi^-)$ model	< 0.01	< 0.01	< 0.01
Background model	< 0.01	< 0.01	< 0.02
Peaking backgrounds	< 0.01	< 0.02	< 0.03
$m(K^+\pi^-\mu^+\mu^-)$ model	< 0.01	< 0.01	< 0.01
$K^+\mu^+\mu^-$ veto	< 0.01	< 0.01	< 0.01
Trigger	< 0.01	< 0.01	< 0.01
Bias correction	< 0.02	< 0.01	< 0.03

Dominant systematics in each observable category

Figure 7: table of systematic uncertainties.

Because of different decays in the same target finalstate, for example $\bar{A}_b^0 \rightarrow \bar{p} \rightarrow \pi^- K^+ \mu\mu$, events that are drawn from distributions of these peaking backgrounds are not taken into the fit. Bias corrections come up if boundary effects

like $F_S > 0$ are required.

$$\frac{d\Gamma}{dq^2}|_{S+P} = (1 - F_S) \frac{d\Gamma}{dq^2}|_P$$

For small F_S the bias towards higher values biases the P-wave and vice versa.

If the energy threshold is so big, that a $c\bar{c}$ pair can be produced in a loop which generates a $J\psi$, the would be a possibility to detect it.

The tension is confirmed with the 2016 data set. The significance of the discrepancy is nuisance parameter dependend and also depends on the q^2 bins.

References

- [1] T. Blake et al. “Round table: Flavour anomalies in $b \rightarrow sl+l-$ processes.” In: *EPJ Web Conf.* 137 (2017). Ed. by Y. Foka, N. Brambilla, and V. Kovalenko, p. 01001. DOI: 10.1051/epjconf/201713701001. arXiv: 1703.10005 [hep-ph].
- [2] Christoph Bobeth, Gudrun Hiller, and Danny van Dyk. “The Benefits of $\bar{B}- > \bar{K}^*l^+l^-$ Decays at Low Recoil.” In: *JHEP* 07 (2010), p. 098. DOI: 10.1007/JHEP07(2010)098. arXiv: 1006.5013 [hep-ph].
- [3] Serguei Chatrchyan et al. “Angular Analysis and Branching Fraction Measurement of the Decay $B^0 \rightarrow K^{*0}\mu^+\mu^-$.” In: *Phys. Lett. B* 727 (2013), pp. 77–100. DOI: 10.1016/j.physletb.2013.10.017. arXiv: 1308.3409 [hep-ex].
- [4] Eluned Anne Smith. *Updated angular analysis of the decay $B^0 \rightarrow K^{*0}(\rightarrow K^+\pi^-)\mu^+\mu^-$* . URL: <https://indi.to/bMm9K> (visited on 07/17/2020).